Unified Methodology to Identify the Potential Application of Seasonal Sorption Storage Technology

Andrea Frazzica [1,*] **, Vincenza Brancato** [1] **and Belal Dawoud** [2]

[1] Consiglio Nazionale delle Ricerche (CNR), Istituto di Tecnologie Avanzate per l'Energia "Nicola Giordano" (ITAE), Via Salita S. Lucia sopra Contesse n. 5, 98126 Messina, Italy; vincenza.brancato@itae.cnr.it

[2] Faculty of Engineering, Laboratory of Sorption Processes, OTH-Regensburg Technical University of Applied Sciences, Galgenberg Street 30, D-93053 Regensburg, Germany; belal.dawoud@oth-regensburg.de

[*] Correspondence: andrea.frazzica@itae.cnr.it; Tel.: +39-090624331

Abstract: In this study, the definition of a new methodology for a preliminary evaluation of the working boundary conditions under which a seasonal thermal energy storage (STES) system operates is described. The approach starts by considering the building features as well as the reference heating system in terms of solar thermal collectors' technology, ambient heat sinks/source, and space heating distribution systems employed. Furthermore, it is based on a deep climatic analysis of the place where the STES needs to be installed, to identify both winter and summer operating conditions. In particular, the STES energy density is evaluated considering different space heating demands covered by the STES (ranging from 10% up to 60%). The obtained results demonstrate that this approach allows for the careful estimation of the achievable STES density, which is varies significantly both with the space heating coverage guaranteed by the STES as well as with the ambient heat source/sink that is employed in the system. This confirms the need for careful preliminary analysis to avoid the overestimation of the STES material volume. The proposed approach was then applied for different climatic conditions (e.g., Germany and Sweden) and the volume of one of the most attractive composite sorbent materials reported in the literature, i.e., multi-wall carbon nanotubes (MWCNT)-LiCl, using water as the working fluid, needed for covering the variable space heating demand in a Nearly Zero Energy Building (NZEB) was calculated. In the case of Swedish buildings, it ranges from about 3.5 m^3 when 10% of the space heating demand is provided by the STES, up to 11.1 m^3 when 30% of the space heating demand is provided by the STES.

Keywords: seasonal thermal storage; composite sorbents; operating conditions

1. Introduction

During the last years, several initiatives have been launched by different countries to further promote the widespread use of renewable sources, aimed at a reduction in the worldwide energy system dependence on fossil fuels [1–4]. The vast majority of the proposed incentives are supporting the increase of renewables' share in the electricity production sector. Indeed, it is recognized that the main pollution sources are represented by the fossil fuels-based big power plants, commonly employed for the centralized production of electricity injected into the electrical grids [5]. Besides the need for reducing the impact of fossil fuels in the electricity generation sector, it has to be considered that, at European level, the heating and cooling sector accounts for about 50% of the overall primary energy consumption of which 75% is still covered by fossil fuels [6]. Indeed, the renewable heating and cooling sectors have been defined as the "sleeping giant" [7], since its further development could help in strongly reducing the overall demand for fossil fuels as well as limiting the exploitation of electricity for the heating and cooling provision.

In such a background, different renewable-based technologies have been proposed for heating and cooling applications in buildings. Among them, the most attractive is represented by solar thermal [8,9] and biomasses [10,11]. Both technologies present the pros and cons. Heating energy produced by solar thermal collectors does not present any pollutant by-product, since they directly convert solar radiation into thermal energy, usually employing a heat transfer fluid (*HTF*) to extract the produced heat. On the other hand, heating production is strongly variable both on a daily and seasonal basis, being dependent on solar availability and radiation intensity. Concerning biomass heating, which is mainly produced through combustion processes, it is characterized by a continuous provision, which is only dependent on biomass availability. Nevertheless, this technology still presents concerns about the emissions related to the combustion process, and, from the life-cycle perspective, it can be highly sustainable only when the biomass comes from nearby production sites (e.g., wooded areas).

To promote the diffusion of solar thermal technology, it is, therefore, necessary to complement the overall system with an optimized thermal energy storage (TES), able to maximize the solar energy exploitation, by shifting the produced thermal energy from the over-production periods (i.e., high solar irradiation availability) to the periods with scarcity or absence of solar availability. Available TES technologies are distinguished by sensible, latent and thermo–chemical [12]. Sensible technology stores thermal energy as a function of the temperature variation of the storage media. Accordingly, the main parameter affecting the overall TES performance is represented by the specific heat. Latent technology mainly exploits the phase transition, usually from solid to liquid and vice-versa, to increase the TES density. For this technology, the crucial parameter is represented by the latent heat associated with the phase transition of the storage media. Thermo–chemical technology exploits reversible physical and chemical reactions to store and release heat. In this case, the heat associated with the reversible reaction represents the main parameter. One of the main features of the thermo–chemical TES compared to both sensible and latent TESs is represented by the possibility of storing thermal energy, virtually, without any energy loss. Indeed, for thermo–chemical TES, the energy is stored as potential energy between two reactants. Accordingly, as long as the reactants are kept separated, the energy is maintained stored. Differently, both sensible and latent TESs lose part of the stored energy due to thermal losses to the surrounding ambient.

In the case of solar thermal heat, it is evident that there is a huge mismatch between the peak of primary source availability, occurring during the summer season, and the peak of energy demand for space heating, occurring during the winter season. This supported the idea of promoting seasonal thermal energy storages (STES), in which the solar energy harvested in summer is kept stored for several months until the heating season begins. The state-of-the-art regarding installed STES is dominated by sensible technology, as recently reported [13]. Currently, sensible STESs are installed in 31 locations in Europe. Mostly, they are based on buried water tanks, sometimes also using gravel. Generally, since the heat losses increase as the surface-to-volume ratio increases, the size of these STESs is quite big and more appropriate for district heating networks and large-scale buildings. To overcome the limitations in achievable storage density and issues related to loss of energy stored during the storage period typical of water-based sensible systems, thermo–chemical STESs were proposed for this application [14]. Indeed, this technology can achieve high storage density, thanks to the high reaction heat, as well as virtually no heat loss during the storage period, thus avoiding TES degradation in the seasonal operation [15,16]. Accordingly, in the last years, several research activities have been devoted to the development of innovative STESs based on the class of thermo–chemical TES. In particular, since the main aim is to drive this technology with standard solar thermal collectors, thus limiting the charging temperature in the range 80–100 °C, sorption technology was identified as the most suitable for STES in buildings. Indeed, sorption, both solid adsorption and liquid absorption, mainly relies on physical and weak chemical bonds, which require limited temperature levels (i.e., below 100 °C) to be split during the charging phase [17]. At the material level, the main activities focus on the development of novel adsorbent materials with enhanced sorption capacity and reduced driving temperature [18]. Particularly, novel composite sorbents, based on a porous structure embedding a hygroscopic salt

were deeply investigated, varying both the porous matrix, i.e., vermiculite [19,20], silica gel [21,22], carbon structures [23,24] and the employed salts, i.e., LiCl, CaCl$_2$, MgSO$_4$, SrBr$_2$ [20–22,24–26]. Some other activities were focused on pure adsorbent materials, belonging to the classical zeolites [27], novel synthetic zeotypes with reduced driving temperature [28], and metal–organic frameworks (MOFs) [29]. Furthermore, design and realization of novel sorption STES reactors, mainly at the lab-scale for validating the technology, were also presented [14–16], demonstrating the feasibility of the proposed concept, but further highlighting the need for design improvement, as well as a better understanding of the system operation.

Even though it is now established that the sorption STES could be a beneficial technology for the further deployment of solar thermal technology in buildings, there is still a lack of methodology in the a-priori evaluation of the potential of novel sorbent materials for this application [30]. Indeed, the sorption TES cannot uniquely be defined by the charging and discharging temperature level (as is done for sensible and latent TESs), since both charging and discharging phases strongly also depend on the ambient conditions, which usually represent the sink to which the condensation energy is rejected during charging and the source from which the evaporation energy is taken during discharging. This means that to have a thorough evaluation of the potential of a given sorption STES, a reliable analysis of the real operating conditions under which a STES operates needs to be performed. So far, the common approach followed to identify the charging and discharging conditions is

- Setting the expected charging temperature according to the employed solar thermal collectors' technology;
- Defining the condensation temperature as the average ambient temperature expected during summer;
- Setting the adsorption temperature according to the distribution systems (e.g., radiators, fan coils, floor heating) used in the building;
- Defining the evaporation temperature as the average ambient temperature during winter.

Such an approach brought to the wide variability of boundary conditions identified by different authors. Indeed, Frazzica and Freni [31] evaluated possible working pairs by varying different operating conditions, but, mostly, identifying 100 °C as the charging temperature coupled to 30 °C as the condensation temperature, with 50 °C as the adsorption temperature coupled to 10 °C as the evaporation temperature. Differently, Grekova et al. [32] proposed the following operating conditions, 75–85 °C and 30 °C as the charging and condensation temperatures, respectively, 35 °C and 10 °C as the discharging and evaporation temperatures, respectively. Furthermore, several authors used boundary operating conditions even far from real applicability, as can be deducted by the review of Fumey et al. [14], which makes the comparison of different materials and systems either impossible or unfair. It also has to be pointed out that all the reported analyses always consider the boundary conditions as constant values, aiming at the development of STESs able to satisfy the entire energy demand for the space heating of a building. This most probably represents a target excessively optimistic both from the economic feasibility point of view as well as from the space constraints that may limit the installation of huge STESs, especially in single-family houses.

Starting from the above-reported analysis, this paper aims at the introduction of the first unified methodology for the evaluation of the potential of sorption STESs under real operating conditions. To this aim, a well-defined approach is followed to identify relevant temperature levels, both during charging and discharging phases, which will vary with the building typology targeted by the application, the solar thermal collectors' technology, the ambient heat rejection/supply technology as well as the desired space-heating fraction to be covered by the STES. This approach, still lacking pure dynamic modelling able to deeply analyse the dynamic behaviour of the system, will represent a reliable basis for the a-priori estimation of the achievable performance of a sorption STES, especially regarding the expected storage density and the space needed to cover a defined fraction of space heating by means of solar energy.

2. System Definition

When the sorption STES technology is investigated, the first distinction must refer to the type of storage technology, which is being analysed. Indeed, sorption TESs can be operated both as a closed or an open system [15]. The former one only exchanges energy with its surroundings, operating under a pure working fluid atmosphere (e.g., water vapour), while the latter one exchanges both energy and mass, usually adsorbing and releasing water vapour from/to the ambient air as a working fluid. Clearly, from the construction point of view, the open sorption TES is less expensive and is easier to be realized, since it does not need any special manufacturing process to guarantee a vacuum-tight system, which is instead required for a closed sorption TES. On the other hand, the open TES is strongly affected by the ambient conditions, since it needs sufficient ambient humidity to achieve reasonable performance, resulting in a limiting factor for wide market penetration, especially in different dry weather locations.

In the present work, the performed analysis is therefore focused on the closed and fixed bed reactor sorption TES application. The reference operating system is depicted in Figure 1. The sorption TES is schematically represented by two vessels connected by an internal valve. On top, the adsorption module, which contains the adsorbent material and the heat exchanger (HEX) to provide and extract heat, is represented. At the bottom, the vessel containing the HEX acting as a condenser and evaporator depending on the operating phase is depicted.
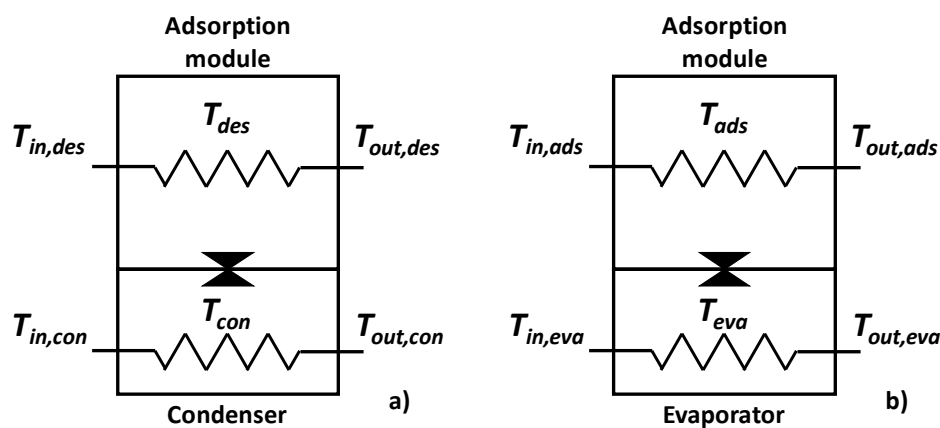

Figure 1. Boundary working conditions for seasonal thermal energy storage (STES) during (**a**) charging phase (i.e., summer season) and (**b**) discharging phase (i.e., winter season).

Given the highly unsteady operating conditions typical of an adsorption system, to take into account the effect of the needed temperature difference between *HTF* and each component, a constant $\Delta T = 5$ K is applied. It will be used to evaluate the most relevant operating conditions of an STES. In particular, the following calculations will be applied:

$$T_{des} = T_{in,des} - \Delta T \tag{1}$$

$$T_{ads} = T_{out,ads} + \Delta T \tag{2}$$

$$T_{con} = T_{in,con} + \Delta T \tag{3}$$

$$T_{eva} = T_{in,eva} - \Delta T \tag{4}$$

To identify the different temperature levels characterising the storage operation, as represented in Figure 2, once the reference building is defined along with the expected space heating and domestic hot water (DHW) demand, the following system characteristics must be defined:

- Solar heat source installed: Once the solar thermal collector technology is defined along with the collectors' field sizing and the climatic conditions in which the system operates, the temperature level that can be delivered to the STES during the charging phase, $T_{in,des}$, can be identified.

- Ambient heat source/heat rejection: Represents the interface between the sorption STES and the ambient. It is needed during the charging phase to dump the condensation heat and during the discharging phase to take up the heat to evaporate the working fluid. It must be optimized considering the climatic conditions under which the system operates. Dry re-coolers/heaters and geothermal probes represent the main possible options, which, along with the climatic conditions, identify both $T_{in,eva}$ and $T_{in,con}$, respectively. Nevertheless, other possibilities, such as exploiting the low-temperature heat from solar thermal collectors in winter (between 10 and 20 °C) to feed the evaporator during the discharging phase, can also be investigated.
- Heat distribution systems: Represent the way in which the produced heat is transferred to the building. Possible technologies are floor heating, fan coils and radiators. According to datasheets and existing design rules and relative standards, it is then possible to identify the temperature needed for each of these technologies to be properly operated, which corresponds to the $T_{out,ads}$.
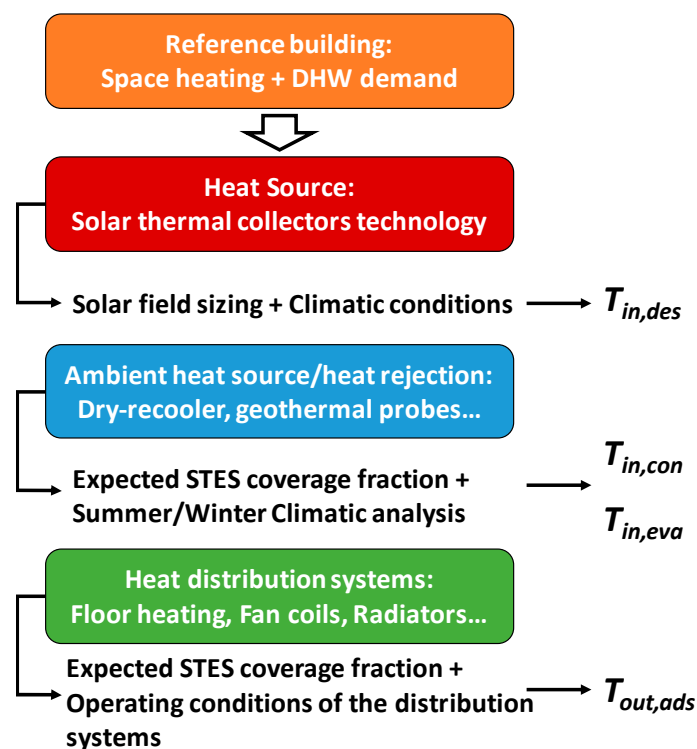

Figure 2. Steps to identify the main operating temperatures of the sorption STES.

Figure 3 schematically represents the reference system considered in the present work, which is the one under development within the European Union (EU) project SWS-Heating. Basically, during the charging phase, solar collectors, connected to a thermal buffer, provide high temperature to the STES to promote the desorption. The heat of condensation is then rejected to the ambient, either through a dry re-cooler or to into the ground by means of geothermal HEX. During the discharging mode, the heat of evaporation can be provided by different sources: ambient heat, through the dry re-cooler, geothermal heat, through the geothermal HEX, solar heat, through the solar thermal collectors. The heat of adsorption is then provided to the distribution system.
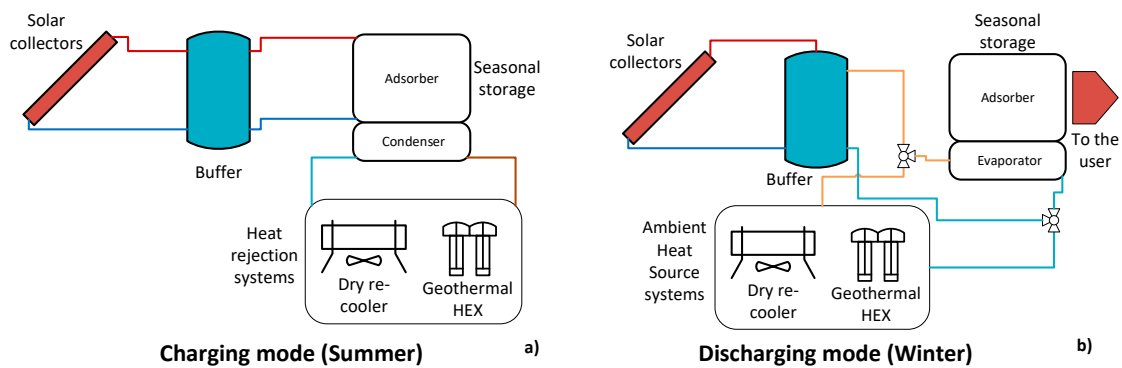
Figure 3. Reference system to which the analysis is applied. Charging mode schematically represented in (**a**) and Discharging mode in (**b**).

Of course, in the present study, the aim is to analyze the operating conditions of the sorbent material. The selection of the most suitable system configuration is an engineering task, dependent on the addressed building, the climatic conditions and also the overall cost of the installation.

The ambient heat source and heat rejection can be estimated by means of a climatic data analysis that will be described in the following section. While the temperature delivered by the solar thermal collectors can be simply set according to the common operating conditions of the different solar thermal collectors' technologies available on the market.

To evaluate the temperature needed for the space heating provision, it is necessary to define the technology adopted. The performed calculations assume floor heating as the heating distribution technology. Indeed, the STES seems more attractive for highly efficient buildings, where floor heating is now the most widely employed technology. Furthermore, for sorption systems, the possibility of operating with low-temperature heating devices is of utmost importance to maximise their efficiency. The definition of the temperature levels of the floor heating distribution system can be performed by following the standards for gas-fired sorption devices [33,34]. In this case, the supply and return temperature of the fluid inside the loop can be calculated defining, as nominal operating conditions, the ones under which the external temperature is the minimum throughout the year, which is defined as the ambient nominal temperature, $T_{a,N}$. Under this condition, the heating power that the floor heating system can deliver is defined as

$$\dot{Q}_{H,N} = \dot{m}_{HTF} cp_{HTF} (T_{S,N} - T_{R,N}) \tag{5}$$

where $\dot{Q}_{H,N}$ represents the provided heating power; $T_{S,N}$ and $T_{R,N}$, the nominal supply and return temperatures of the hydraulic *HTF* loop, respectively. This power represents the maximum power that needs to be delivered by the floor heating distribution system since it is calculated under the most critical external condition. To evaluate how the power changes at higher external temperatures, again, the procedure suggested in [33,34] needs to be followed, coupled to the evaluation of the heating capacity, which can be provided by the specific floor heating system, according to the EN 442-2 [35]. Out of this, a characteristic heating capacity can be calculated, defined as the part-load ratio (*PLR*), according to the following:

$$PLR(T_a) = \frac{\dot{Q}_H(T_a)}{\dot{Q}_{H,N}} = \left[\frac{\overline{T}_{HTF}(T_a) - T_{room}}{\overline{T}_{HTF,N} - T_{room}} \right]^n \tag{6}$$

It represents the ratio between the actual heating power needed at the given ambient temperature, $\dot{Q}_H(T_a)$, and the nominal heating power calculated under the most severe conditions, $\dot{Q}_{H,N}$. These powers are represented by the difference between the average *HTF* temperature inside the loop, $\overline{T}_{HTF}$, and the reference design temperature of the heated room, T_{room}, commonly set at 20 °C. The

exponential factor, *n*, characterizes the specific floor heating system and usually varies between 0.9 and 1.1. Assuming a floor heating system with *n* = 1, basically, the *PLR* has a linear trend between the maximum power, $\dot{Q}_{H,N}$, and the minimum power, which is equal to zero, when the ambient temperature is exactly the same as the set heating temperature, T_{room}. Figure 4 represents a reference example of the *HTF* temperature evolution, namely, supply, average and return temperature, obtained for a case where $T_{a,N}$ = −15 °C, $T_{S,N}$ = 38 °C and $T_{R,N}$ = 28 °C.
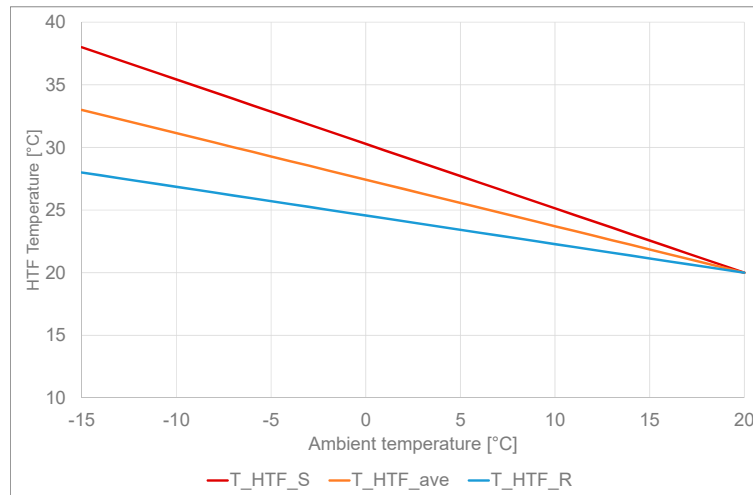

Figure 4. Supply, return and average heat transfer fluid (*HTF*) temperature as a function of ambient temperature for a reference case with $T_{a,N}$ = −15 °C, $T_{S,N}$ = 38 °C and $T_{R,N}$ = 28 °C.

To calculate the *HTF* temperature variation to provide the heating energy to the building as a function of the *PLR* defined above, considering a linear decrease from the nominal values down to the set room temperature, the following Equation (7) can be defined.

$$T_{HTF}(T_a) = T_{room} + (T_{HTF,N} - T_{room})\,PLR(T_a) \tag{7}$$

From this, the supply temperature corresponding to the $T_{out,ads}$ that must be delivered by the STES, can be calculated by means of the following Equation (8), considering that also the ΔT between supply and return temperature of the *HTF* will be characterized by a linear dependency to the *PLR*.

$$T_S(T_a) = T_{HTF}(T_a) + \frac{T_{S,N} - T_{R,N}}{2}\,PLR(T_a) \tag{8}$$

Clearly, there is an ambient temperature limit above which there is no need to provide heating through the floor heating system, as the internal heat gains together with the solar gains through windows do compensate for the heat losses through the building's envelope as well as the ventilation and infiltration losses. A typical value for such a heating limit temperature in passive houses and Nearly Zero Energy Building (NZEB) in Europe is 10° C. For this reason, as will be presented in the following section, the space heating demand is evaluated on a yearly basis only when the ambient temperature falls below 10 °C.

3. Climatic Data Analysis

Most of the temperature boundary conditions, as well as the evaluation of the heating load distribution, can only be calculated by performing an accurate climatic data analysis. Indeed, if, on the one hand, the external temperatures for condensation and evaporation can be extracted from this analysis, on the other hand, the temperature distribution during the heating season can be correlated to the specific heating demand distribution. Indeed, the heating demand of a building is proportional

to the temperature difference between the internal set-point temperature and the ambient temperature. Accordingly, knowing the hourly ambient temperature distribution, the specific heat demand can be easily calculated.

The proposed approach is described for two reference climates, namely, Stockholm (Sweden) and Regensburg (Germany), representing typical northern and central European climatic conditions. Starting from a common climatic database, Meteonorm 7.0 [36], in this case, the yearly temperature distribution can be evaluated, as reported in Figure 5. Starting from these values, it is possible to rank the number of hours of the year in which a specific ambient temperature is registered. Referring only to the winter season, and specifically to the ambient temperature up to 10 °C, which is considered as the external temperature limit for a well-insulated building above which no space heating provision is needed, the temperature distribution per hours, as well as the cumulative one, are represented in Figures 6a and 7a for Stockholm and Regensburg, respectively. To make the calculation accurate enough but easy to perform, the distribution was extrapolated by clustering the data obtained from the climatic analysis every 1 °C. This means that, referring to Figures 6a and 7a, the relative ambient temperature distribution at 5 °C is obtained by summing the number of hours of the year during which the temperature falls between 4.1 °C and 5 °C. Since the heating demand is proportional to the difference between the internal set-point temperature and the ambient temperature, starting from the temperature distribution, the heating demand was calculated for each ambient temperature as

$$Q_H = n_{hours}(T_{room} - T_a) \tag{9}$$

where n_{hours} represents the number of hours during which the ambient temperature, T_a, is registered, while T_{room} represents the internal set-point, considered as 20 °C. Figures 6b and 7b represent the relative and cumulative distribution for the heating demand calculated according to Equation (9) for Stockholm and Regensburg, respectively. As expected, the two trends were similar, even if, for the heating demand calculation, the relative weight of the low ambient temperature conditions was slightly enhanced. In both cases, the highest relative heating demand was concentrated in an ambient temperature range between 0 °C and 5 °C, even if, for Stockholm, relevant heating demand was also concentrated slightly below 0 °C.
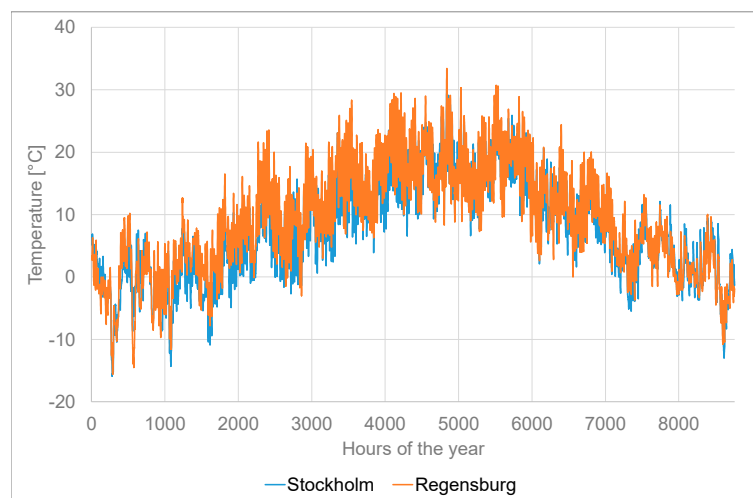

Figure 5. Hourly ambient temperature evolution for a reference year in Stockholm (Sweden) and Regensburg (Germany), evaluated from the Meteonorm 7.0 database.
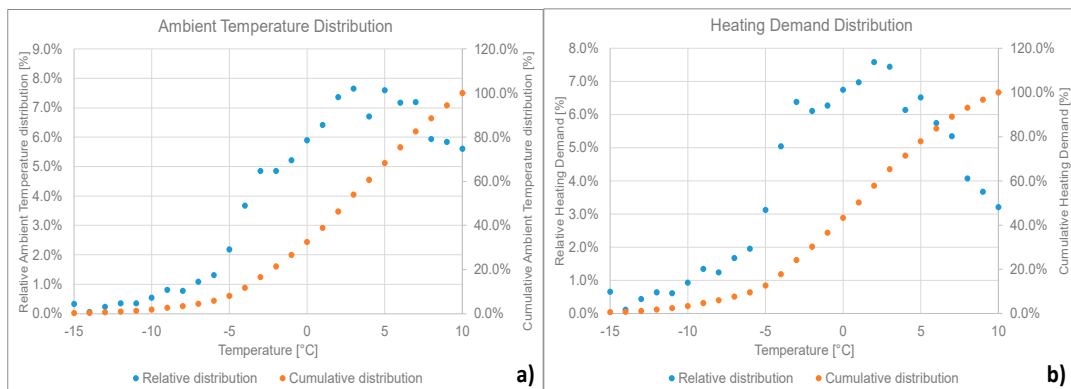
Figure 6. Ambient temperature distribution for the heating season in Stockholm (**a**) and heating demand derived from the climatic analysis (**b**).
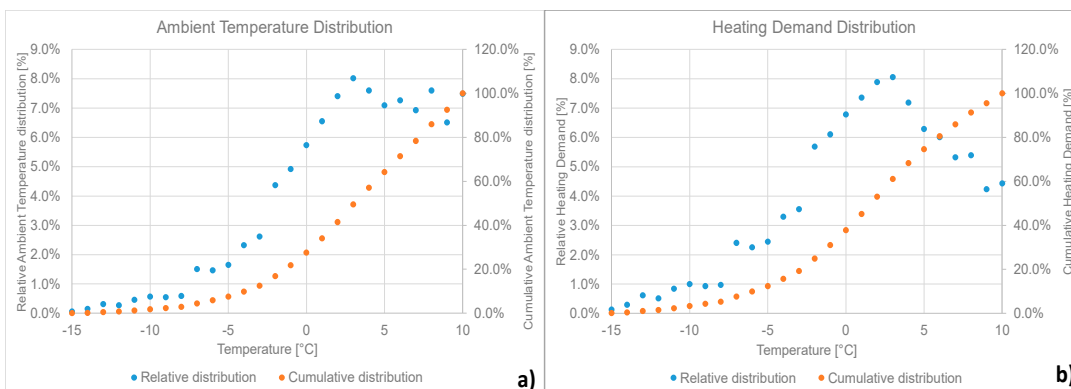

Figure 7. Ambient temperature distribution for the heating season in Regensburg (**a**) and heating demand derived from the climatic analysis (**b**).

4. Identification of Reference Boundaries

In this section, two examples of calculation of reference boundary conditions are reported for the two cities reported above, namely, Regensburg, in Germany, and Stockholm, in Sweden, considering the possible heating system reported in Figure 3.

The reference boundaries are obtained following the steps proposed in Figure 2. For what concerns the summer charging phase, the charging temperature, T_{in_des}, was fixed as 90 °C, considering the use of evacuated tube solar collectors to drive the desorption process. Since to size the solar collectors' field, a dynamic simulation is needed. In this preliminary analysis, the assumption was that the sizing of the solar field was enough to provide the needed energy to charge the STES.

To define the inlet condensation temperature, $T_{in,con}$, the ambient temperature evolution registered during the two warmest months of the year (i.e., from the second half of June up to the end of August) were analysed, as reported in Figure 8. For this analysis, given the high variability of the temperature, it was necessary to define an average ambient temperature as a reference. The average ambient temperature was calculated for these months as the average temperature occurring during the daytime since this represents the charging period. The obtained values were about 20 °C for Stockholm and 23 °C for Regensburg. Considering a $\Delta T = 5$ K between the ambient air and the *HTF*, the identified conditions were then $T_{in,con} = 28$ °C for Regensburg and $T_{in,con} = 25$ °C for Stockholm. Furthermore, the operation of the geothermal *HEX* as the heat rejection system during the charging phase was also considered. In this case, the reference inlet temperature needed to be evaluated depending on the sizing of the geothermal *HEX*. For this example, a $T_{in,con} = 22$ °C was assumed.
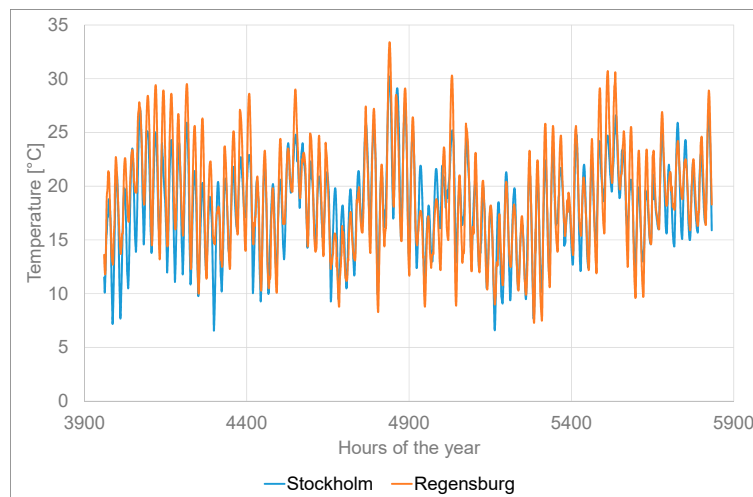
Figure 8. Ambient temperature evolution for the two hot summer months (second half of June, July, and August) for Stockholm and Regensburg.

Concerning the definition of the inlet evaporation temperature, it strongly depends on which system is implemented to provide energy to the evaporator. Indeed, as can be argued from the ambient temperature evolution reported for both cities in Figure 5, specifically for the cold months, most of the time, the temperature is close or below 5 °C in the case of Regensburg and even colder for Stockholm. Since water is the commonly employed working fluid, to operate the STES and avoid freezing issues inside the evaporator, an inlet temperature of at least 10 °C is needed. To achieve this target, two main options can be pursued, either exploiting the low-temperature heat provided by the solar collectors' field in wintertime, ranging between 10 °C and 20 °C, or coupling the storage to geothermal boreholes, able to provide about 10 °C throughout the season. Within the SWS-Heating project activities, the possibility of feeding the evaporator with solar heat gathered during winter has been validated through dynamic simulations performed for different locations. Nevertheless, the exact amount of heat that can be harvested and used for this purpose needs to be quantified once the overall system is designed. Since the most effective solution can only be defined through a detailed sizing coupled to dynamic modelling, three different scenarios were considered to evaluate the potentiality of the STES materials:

- Scenario 1. System exploiting only solar heat and ambient heat through the dry re-cooler: The evaporation energy is provided either at $T_{in,ev} = 15$ °C or $T_{in,ev} = 10$ °C, depending on the ambient temperature and solar availability. The condensation heat is represented by the average ambient temperature in summer-time, as described in Figure 8;
- Scenario 2. System based on the geothermal *HEX* both as the ambient source and sink during winter and summer, respectively. In this case, $T_{in,ev} = 10$ °C, while $T_{in,con} = 23$ °C throughout the operation;
- Scenario 3. Mixed system, in which the evaporation energy exploits the higher temperature possible, i.e., either $T_{in,ev} = 10$ °C or $T_{in,ev} = 15$ °C, depending on the ambient conditions, while the condensation heat is dissipated through the geothermal HEX, guarantying a constant $T_{in,con} = 23$ °C.

Finally, to identify the temperature to be delivered to the space heating distribution system, $T_{out,ads}$, both the target STES coverage fraction that needs to be achieved as well as the cumulative space heating distribution for the climatic location must be defined. Indeed, depending on the expected STES coverage fraction, it is possible to identify the corresponding ambient temperature range and, consequently, the $T_{out,ads}$, which corresponds to the supply temperature of the *HTF* of the floor heating, as represented in Figure 4.

The analyses for the heating demand distribution are the ones reported in Figures 6b and 7b for Stockholm and Regensburg, respectively.

Starting from the performed climatic analyses, the following correspondence between the STES coverage fractions, which represent the energy that needs to be stored and delivered by the STES, the ambient temperatures and the floor heating supply temperature can be obtained. In particular, Table 1 summarizes the outcomes achieved for Stockholm, while Table 2 the ones obtained for Regensburg. The applied methodology was as follows: Once a relative heating demand coverage was selected, e.g., 20%, referring to Figures 6 and 7, the corresponding temperature range was identified. For instance, 20% of the heating demand is occurring in the ambient temperature range between 6 °C and 10 °C, both for Regensburg and Stockholm. Subsequently, the amount of heating demand corresponding to each ambient temperature was calculated and the relative energy needed for each ambient temperature was calculated by dividing it by the overall heating energy needed to achieve the identified 20% of heating demand coverage. This procedure was applied to all the investigated heating demand coverages. Finally, corresponding to each ambient temperature, the expected $T_{out,ads}$ to provide space heating through the floor heating system was also defined according to the evolution reported in Figure 4.

Table 1. Analysis of the heating distribution as a function of the expected seasonal thermal energy storage (STES) coverage fraction, for Stockholm. The table also reports the ambient temperature and the relative supply temperature needed by the floor heating system.

	STES Coverage Fraction						
	10%	**20%**	**30%**	**40%**	**50%**	**60%**	
T_a [°C]	Relative Heating Demand Covered						$T_{out,ads}$ [°C]
10	32.1%	16.0%	10.7%	8.0%	6.4%	5.3%	25.1
9	36.7%	18.4%	12.2%	9.2%	7.3%	6.1%	25.7
8	31.2%	20.4%	13.6%	10.2%	8.1%	6.8%	26.2
7	–	26.7%	17.8%	13.4%	10.7%	8.9%	26.7
6	–	18.5%	19.1%	14.4%	11.5%	9.6%	27.2
5	–	–	21.7%	16.3%	13.0%	10.9%	27.7
4	–	–	4.8 %	15.4%	12.3%	10.2%	28.2
3	–	–	–	13.2%	14.9%	12.4%	28.7
2	–	–	–	–	15.2%	12.6%	29.3
1	–	–	–	–	0.5%	11.6%	29.8
0	–	–	–	–	–	5.5%	30.3

Table 2. Analysis of the heating distribution as a function of the expected STES coverage fraction, for Regensburg. The table also reports the ambient temperature and the relative supply temperature needed by the floor heating system.

	STES Coverage Fraction						
	10%	**20%**	**30%**	**40%**	**50%**	**60%**	
T_a [°C]	Relative Heating Demand Covered						$T_{out,ads}$ [°C]
10	44.3%	22.1%	14.8%	11.1%	8.5%	7.4%	25.1
9	42.3%	21.2%	14.1%	10.6%	10.8%	7.1%	25.7
8	13.4%	27.0%	18.0%	13.5%	10.6%	9.0%	26.2
7	–	26.6%	17.7%	13.3%	12.0%	8.9%	26.7
6	–	3.1%	20.0%	15.0%	12.6%	10.0%	27.2
5	–	–	15.4%	15.7%	14.4%	10.5%	27.7
4	–	–	–	18.0%	16.1%	12.0%	28.2
3	–	–	–	2.8%	15.0%	13.4%	28.7
2	–	–	–	–	–	13.1%	29.3
1	–	–	–	–	–	8.7%	29.8

To minimize the variability of the supply temperature to be considered throughout the heating season, the $T_{out,ads}$ reported in Tables 1 and 2 were clustered to the corresponding upper integer value. For instance, analysing Table 2, for the STES coverage fraction equal to 20%, the identified $T_{out,ads}$ of 25.1 °C and 25.7 °C, were considered equal to 26 °C, with a corresponding relative heating demand of 43.3%, obtained by summing the relative heating demands calculated for 25.1 °C and 25.7 °C.

According to this approach, the floor heating supply temperatures and the relative heating demand covered for the different STES coverage fractions are summarized in Tables 3 and 4, for Stockholm and Regensburg, respectively. As can be analysed, in both cases, high supply temperature, e.g., 30 °C, is only needed when a high STES coverage fraction is requested, i.e., 50% for Stockholm and 60% for Regensburg. Furthermore, as expected, given the colder northern European climate, the share of energy supply at higher $T_{out,ads}$ is more pronounced in Stockholm rather than Regensburg. This reflects on the achievable STES energy storage density.

Table 3. Defined space heating supply temperatures for different STES coverage fraction coverage in Stockholm.

STES Coverage Fraction	Floor Heating Supply Temperature, $T_{out,ads}$ [°C]					
	26	**27**	**28**	**29**	**30**	**31**
10%	68.8%	31.2%	–	–	–	–
20%	34.4%	47.1%	18.5%	–	–	–
30%	22.9%	31.4%	40.9%	4.8%	–	–
40%	17.2%	23.6%	30.7%	28.6%	–	–
50%	13.8%	18.8%	24.5%	27.2%	15.7%	–
60%	11.5%	15.7%	20.4%	22.6%	24.3%	5.5%
	Relative heating demand covered					

Table 4. Defined space heating supply temperatures for different solar fraction coverage in Regensburg.

STES Coverage Fraction	Floor Heating Supply Temperature, $T_{out,ads}$ [°C]				
	26	**27**	**28**	**29**	**30**
10%	86.6%	13.4%	–	–	–
20%	43.3%	53.6%	3.1%	–	–
30%	28.9%	35.7%	35.4%	–	–
40%	21.7%	26.8%	30.8%	20.8%	–
50%	19.2%	22.7%	27.0%	31.1%	–
60%	14.4%	17.9%	20.5%	25.4%	21.8%
	Relative heating demand covered				

To complete this analysis, the reference boundaries were obtained considering the inlet conditions defined above as well as Equations (1)–(4) reporting the needed ΔT to be considered for a proper heat transfer inside each component. T_{des}, T_{con} and T_{eva} are summarized in Table 5 for both Stockholm and Regensburg, while the T_{ads} can be calculated from the values reported in Tables 3 and 4 applying the Equation (2) to consider the needed ΔT.

Table 5. Reference STES boundaries for Regensburg and Stockholm.

Location	T_{des} [°C]	T_{con} [°C]		T_{eva} [°C]	
Stockholm	85	30 (dry re-cooler)	28 (geothermal HEX)	5 (geothermal HEX)	10 (solar heat)
Regensburg	85	33 (dry re-cooler)	28 (geothermal HEX)	5 (geothermal HEX)	10 (solar heat)

5. Potential Assessment of Different Working Pairs for STES Application

Starting from the boundary conditions defined in the previous sections, the potential application of some adsorbent working pairs reported in the literature is analysed. In particular, the analysis is performed following the approach for the STES density calculation applied in [31], while the two most promising working pairs there reported, namely, MWCNT-LiCL and AQSOA Z02, with water as the working fluid are considered. The former one is a composite sorbent, using multi-wall carbon nanotubes (MWCNT) as a support matrix and LiCl as hygroscopic salt [23], while the latter one is a pure adsorbent material, belonging to the zeotype family [28]. The three scenarios reported above are evaluated.

The obtained results for Scenario 1, system without geothermal HEX, are summarized in Figure 9, while Figure 10 summarizes the obtained results for Scenario 2, system using only geothermal HEX as the ambient heat source/sink and Scenario 3, system using geothermal HEX as the ambient sink and the highest possible temperature as the ambient source for evaporation.
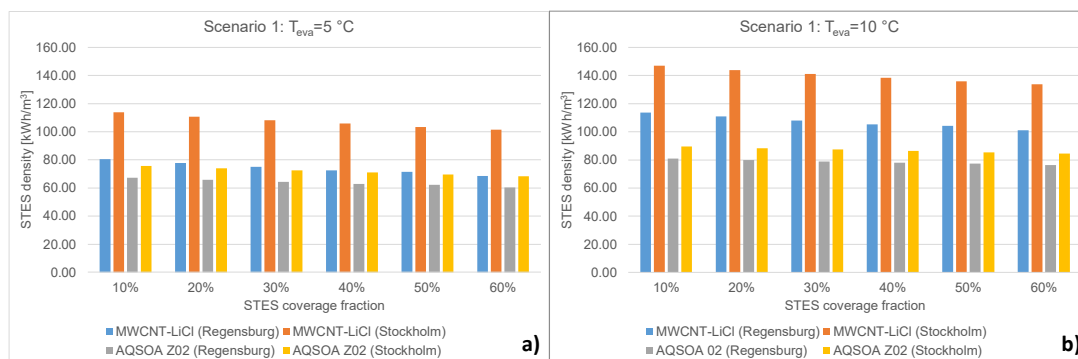

Figure 9. STES energy density calculated for Scenario 1 with evaporation temperature set at 5 °C (**a**) and Scenario 1 with evaporation temperature set at 10 °C (**b**), for the identified working pairs (i.e., multi-wall carbon nanotubes (MWCNT)-LiCl/water and AQSOA 02/water), both in Regensburg and Stockholm.
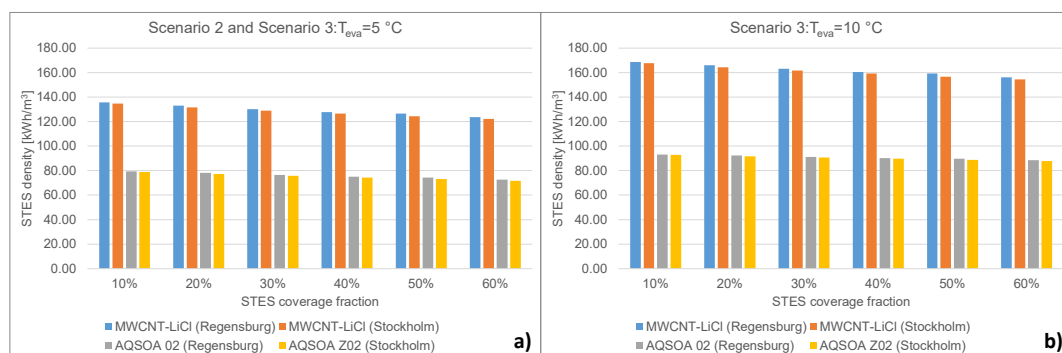

Figure 10. STES energy density calculated for Scenario 2 corresponding also to Scenario 3 with evaporation temperature set at 5 °C (**a**) and Scenario 3 with evaporation temperature set at 10 °C (**b**), for the identified working pairs (i.e., MWCNT-LiCl/water and AQSOA 02/water), both in Regensburg and Stockholm.

Analysing the obtained results for Scenario 1, it is evident that the STES densities for Stockholm were always higher than their corresponding values for Regensburg, which can be solely explained by the lower condenser temperature (30 compared to 33 °C), as summarized in Table 5. Differently, for Scenario 2 and Scenario 3, since the condensation temperature is the same, the obtained deviation is only due to the discharging temperature, whose relative weight was much lower, due to the similar ambient conditions of the two investigated cities. Comparing Scenario 3 to Scenario 1 at the same

evaporation temperature, it is clear that the Scenario 3 always guarantees an increase in STES density of about 15–20%. This is due to the lower condensation temperature during the charging phase.

Some further interesting analyses can be performed out of the obtained results. As expected, the composite sorbent MWCNT-LiCl always gets higher STES energy density compared to the pure adsorbent AQSOA 02, since the differential water uptake is increased due to the presence of the hygroscopic salt. Furthermore, the effect of the evaporation temperature also enhances the STES density up to 45% passing from 5 °C to 10 °C. The most interesting outcome that confirms the usefulness of this unified approach is that varying the STES expected coverage space heating fraction, the energy storage density varies, and this is something that was never reported before, but it is of primary importance to preliminary sizing the STES. For instance, referring to Scenario 1, the energy density when 10% of the space heating needs are covered by the STES is up to 20% higher than the density achievable when 60% of the space heating needs are covered by the STES. The effect of this analysis is even more important when comparing the STES density that can be estimated with this proposed approach against the typical approaches reported in the literature [28,30,31], where, usually, fixed temperature boundary conditions are considered, regardless of the ambient temperature variability typical of each climatic zone. Indeed, considering, for instance, a constant $T_{ads} = 35\,°C$ for providing space heating throughout the winter, when the STES coverage fraction is 60%, the evaluated density is underestimated in a range between 10% and 40%, depending on the working pair and scenario analysed.

An estimation of the adsorbent material volume needed to cover the space heating demand of an NZEB can be performed, considering as reference space heating demand 40 kWh/m^2 y, in line with the Swedish standard [37] and a residential building of 120 m^2. For the Swedish case, Scenario 2 is considered as a target, due to the very low ambient temperature and solar irradiation typical of Northern European countries. For the German one, Scenario 1 is considered, assuming an even evaporation temperature distribution between 5 °C and 10 °C. The obtained results are summarized in Table 6.

Table 6. Expected volume of multi-wall carbon nanotubes (MWCNT)-LiCl and AQSOA, to cover different space heating energy demand for NZEB in residential Swedish and German buildings.

Location	Sorbent Material	STES Coverage Fraction					
		10%	20%	30%	40%	50%	60%
Stockholm $T_{des} = 85\,°C$ $T_{con} = 28\,°C$ $T_{eva} = 5\,°C$	MWCNT-LiCl volume [m^3]	3.57	7.20	11.16	15.17	19.32	23.58
	AQSOA 02 volume [m^3]	6.09	12.43	18.99	25.18	32.89	40.19
Regensburg $T_{des} = 85\,°C$ $T_{con} = 33\,°C$ $T_{eva} = 5{-}10\,°C$	MWCNT-LiCl volume [m^3]	4.94	10.18	15.73	21.59	27.33	33.97
	AQSOA 02 volume [m^3]	6.48	13.18	20.11	27.29	34.38	42.17

It is evident that still a quite huge volume of the sorbent material is needed to cover relevant fractions of space heating demands. Nevertheless, especially for the composite sorbent MWCNT-LiCl, this is also related to the very low density (i.e., 300 kg/m^3), which increases the volume needed despite the very high gravimetric energy density. It is also clear that, for instance, in Regensburg, using Scenario 2 based on the geothermal HEX, a further reduction in the needed material of about 30% compared to the results reported in Table 6 can be achieved. This further stresses the importance of selecting the proper material coupled to the best performing system configuration, to achieve the highest performance.

It has to be pointed out that the performed calculations assume only the portion of space heating covered by the STES, while, considering the solar field-installed, as well as the low temperature required for space heating, a certain fraction of space heating can be covered during winter by directly exploiting solar radiation. In such a way, the share of renewables for heating purposes can be enhanced

reducing the amount of sorbent material needed. Furthermore, given the huge amount of adsorbent material needed for this application, and the possible space constraints in a single-family house, this technology can be of interest for multi-family houses application also, where more space could be available for this kind of installation. It has to be considered that the volume of material calculated according to the proposed methodology does not represent the volume occupied by the STES system. Indeed, the space needed for the HEXs, the vacuum vessel and the evaporator/condenser needs to be added to achieve the final volume of the installation. This depends on the proper sizing and design activity of the technology.

6. Conclusions

A novel methodology to define the reference boundary conditions for a-priori evaluating the volume of material needed to cover the space heating demand of a building was presented. Differently from the other literature analyses, this approach focuses on carefully analysing the climatic conditions under which the STES operates as well as the reference system (i.e., solar thermal collectors' technology, ambient sources/sinks and space heating distribution systems). Furthermore, the analysis considers the variable space heating demand, which can be covered by the STES, ranging between 10% and 60%. Such a unified methodology demonstrated that the achievable STES energy density varies up to 20% when the STES coverage fraction ranges from 10% to 60%, simply because the ambient conditions vary a lot throughout the heating season, thus affecting the temperature that needs to be delivered by the STES to the building. This method is of primary importance to avoid overestimation of the required amount of adsorbent material for STES applications and of course, also drives possible improvement in the management strategies of such a technology, pointing out the importance of selecting the best ambient conditions during which the discharging phase needs to be performed in winter. Furthermore, it can also be used to make an evaluation of the achievable performance of an STES under controlled boundary conditions during lab testing development activities.

Author Contributions: Conceptualization, A.F. and B.D.; Data curation, V.B. and B.D.; Formal analysis, A.F.; Funding acquisition, A.F. and B.D.; Methodology, V.B. and B.D.; Writing – original draft, A.F.; Writing – review and editing, V.B. and B.D. All authors have read and agreed to the published version of the manuscript.

Conflicts of Interest: The authors declare no conflict of interest.

Nomenclature

c_p	Specific heat at constant pressure, kJ/(kg·K)
$\dot{m}$	Mass flow rate, kg/s
n	Number and exponent in equation 6
Q	Heating demand, kJ
$\dot{Q}$	Heating power, kW
T	Temperature, °C or K
$\overline{T}$	Average temperature, °C

Greek letters

Δ	Differential operator

Subscripts

a	average
ads	Adsorption
con	Condenser
des	Desorption
eva	Evaporator
H	Heating

HTF	Heat transfer fluid
in	Inlet
N	Nominal
out	Outlet
room	room
R	Return
S	Supply

Abbreviations

DHW	Domestic Hot Water
HEX	Heat Exchanger
HTF	Heat Transfer Fluid
MOF	Metal-Organic Framework
PLR	Part Load Ratio
STES	Seasonal Thermal Energy Storage
TES	Thermal Energy Storage

References

1. Aquila, G.; de Pamplona, E.O.; de Queiroz, A.R.; Rotela, P., Jr.; Fonseca, M.N. An overview of incentive policies for the expansion of renewable energy generation in electricity power systems and the Brazilian experience. *Renew. Sustain. Energy Rev.* **2017**, *70*, 1090–1098. [CrossRef]
2. Zhao, Z.-Y.; Chen, Y.-L.; Chang, R.-D. How to stimulate renewable energy power generation effectively? – China's incentive approaches and lessons. *Renew. Energy* **2016**, *92*, 147–156. [CrossRef]
3. Abu-Bakar, S.H.; Muhammad-Sukki, F.; Ramirez-Iniguez, R.; Munir, A.B.; Mohd Yasin, S.H.; Mallick, T.K.; McLennan, C.; Rahim, R.A. Financial analysis on the proposed renewable heat incentive for residential houses in the United Kingdom: A case study on the solar thermal system. *Energy Policy* **2014**, *65*, 552–561. [CrossRef]
4. Matschoss, P.; Bayer, B.; Thomas, H.; Marian, A. The German incentive regulation and its practical impact on the grid integration of renewable energy systems. *Renew. Energy* **2019**, *134*, 727–738. [CrossRef]
5. Gaete-Morales, C.; Gallego-Schmid, A.; Stamford, L.; Azapagic, A. Life cycle environmental impacts of electricity from fossil fuels in Chile over a ten-year period. *J. Clean. Prod.* **2019**, *232*, 1499–1512. [CrossRef]
6. European Commission. *An EU Strategy on Heating and Cooling*; European Commission: Brussels, Belgium, 2016.
7. European Renewable Energy Council. *Re-thinking 2050-A 100% Renewable Energy Vision for the European Union*; EREC: Brussels, Belgium, 2010.
8. Evangelisti, L.; De Lieto Vollaro, R.; Asdrubali, F. Latest advances on solar thermal collectors: A comprehensive review. *Renew. Sustain. Energy Rev.* **2019**, *114*, 109318. [CrossRef]
9. Choi, Y.; Mae, M.; Roh, H.; Cho, W. Annual Heating and Hot Water Load Reduction Effect of Air-Based Solar Heating System Using Thermal Simulation. *Energies* **2019**, *12*, 1054. [CrossRef]
10. Wegener, M.; Malmquist, A.; Isalgué, A.; Martin, A. Biomass-fired combined cooling, heating and power for small scale applications—A review. *Renew. Sustain. Energy Rev.* **2018**, *96*, 392–410. [CrossRef]
11. Las-Heras-Casas, J.; López-Ochoa, L.M.; Paredes-Sánchez, J.P.; López-González, L.M. Implementation of biomass boilers for heating and domestic hot water in multi-family buildings in Spain: Energy, environmental, and economic assessment. *J. Clean. Prod.* **2018**, *176*, 590–603. [CrossRef]
12. Lizana, J.; Chacartegui, R.; Barrios-Padura, A.; Valverde, J.M. Advances in thermal energy storage materials and their applications towards zero energy buildings: A critical review. *Appl. Energy* **2017**, *203*, 219–239. [CrossRef]
13. Bott, C.; Dressel, I.; Bayer, P. State-of-technology review of water-based closed seasonal thermal energy storage systems. *Renew. Sustain. Energy Rev.* **2019**, *113*. [CrossRef]
14. Fumey, B.; Weber, R.; Baldini, L. Sorption based long-term thermal energy storage—Process classification and analysis of performance limitations: A review. *Renew. Sustain. Energy Rev.* **2019**, *111*, 57–74. [CrossRef]
15. Palomba, V.; Frazzica, A. Recent advancements in sorption technology for solar thermal energy storage applications. *Sol. Energy* **2019**, *192*, 69–105. [CrossRef]

16. Scapino, L.; Zondag, H.A.; Van Bael, J.; Diriken, J.; Rindt, C.C.M. Sorption heat storage for long-term low-temperature applications: A review on the advancements at material and prototype scale. *Appl. Energy* **2017**, *190*, 920–948. [CrossRef]

17. Aristov, Y.I. Adsorptive transformation of heat: Principles of construction of adsorbents database. *Appl. Therm. Eng.* **2012**, *42*, 18–24. [CrossRef]

18. Cabeza, L.F.; Solé, A.; Barreneche, C. Review on sorption materials and technologies for heat pumps and thermal energy storage. *Renew. Energy* **2017**, *110*, 3–39. [CrossRef]

19. Zhang, Y.; Wang, R.; Li, T.; Zhao, Y. Thermochemical Characterizations of Novel Vermiculite-LiCl Composite Sorbents for Low-Temperature Heat Storage. *Energies* **2016**, *9*, 854. [CrossRef]

20. Brancato, V.; Gordeeva, L.G.; Sapienza, A.; Palomba, V.; Vasta, S.; Grekova, A.D.; Frazzica, A.; Aristov, Y.I. Experimental characterization of the LiCl/vermiculite composite for sorption heat storage applications. *Int. J. Refrig.* **2019**, *105*, 92–100. [CrossRef]

21. Courbon, E.; D'Ans, P.; Permyakova, A.; Skrylnyk, O.; Steunou, N.; Degrez, M.; Frère, M. A new composite sorbent based on SrBr2 and silica gel for solar energy storage application with high energy storage density and stability. *Appl. Energy* **2017**, *190*, 1184–1194. [CrossRef]

22. Yu, N.; Wang, R.Z.; Lu, Z.S.; Wang, L.W. Development and characterization of silica gel-LiCl composite sorbents for thermal energy storage. *Chem. Eng. Sci.* **2014**, *111*, 73–84. [CrossRef]

23. Grekova, A.; Gordeeva, L.; Aristov, Y. Composite sorbents "Li/Ca halogenides inside Multi-wall Carbon Nano-tubes" for Thermal Energy Storage. *Sol. Energy Mater. Sol. Cells* **2016**, *155*, 176–183. [CrossRef]

24. Wang, J.Y.; Wang, R.Z.; Wang, L.W. Water vapor sorption performance of ACF-CaCl2 and silica gel-CaCl2 composite adsorbents. *Appl. Therm. Eng.* **2016**, *100*, 893–901. [CrossRef]

25. Yu, N.; Wang, R.Z.; Lu, Z.S.; Wang, L.W. Study on consolidated composite sorbents impregnated with LiCl for thermal energy storage. *Int. J. Heat Mass Transf.* **2015**, *84*, 660–670. [CrossRef]

26. Ristić, A.; Maučec, D.; Henninger, S.K.; Kaučič, V. New two-component water sorbent CaCl2-FeKIL2 for solar thermal energy storage. *Microporous Mesoporous Mater.* **2012**, *164*, 266–272. [CrossRef]

27. Fischer, F.; Lutz, W.; Buhl, J.-C.; Laevemann, E. Insights into the hydrothermal stability of zeolite 13X. *Microporous Mesoporous Mater.* **2018**, *262*, 258–268. [CrossRef]

28. Brancato, V.; Frazzica, A. Characterisation and comparative analysis of zeotype water adsorbents for heat transformation applications. *Sol. Energy Mater. Sol. Cells* **2018**, *180*, 91–102. [CrossRef]

29. Gordeeva, L.G.; Solovyeva, M.V.; Aristov, Y.I. NH2-MIL-125 as a promising material for adsorptive heat transformation and storage. *Energy* **2016**, *100*, 18–24. [CrossRef]

30. Palomba, V.; Frazzica, A. Comparative analysis of thermal energy storage technologies through the definition of suitable key performance indicators. *Energy Build.* **2019**, *185*, 88–102. [CrossRef]

31. Frazzica, A.; Freni, A. Adsorbent working pairs for solar thermal energy storage in buildings. *Renew. Energy* **2017**, *110*, 87–94. [CrossRef]

32. Grekova, A.D.; Gordeeva, L.G.; Aristov, Y.I. Composite "LiCl/vermiculite" as advanced water sorbent for thermal energy storage. *Appl. Therm. Eng.* **2017**, *124*, 1401–1408. [CrossRef]

33. VDI 4650-2. Simplified method for the calculation of the annual heating energy ratio and the annual gas utilisation efficiency of sorption heat pumps. In *Gas Heat Pumps for Space Heating and Domestic Hot Water Production*; Beuth Verlag GmbH: Berlin, Germany, 2013.

34. EN 12309-7:2014. Gas-fired sorption appliances for heating and/or cooling with a net heat input not exceeding 70 kW. In *Part 7: Specific Provisions for Hybrid Appliances*; Comite Europeen de Normalisation: Brussels, Belgium, 2014.

35. EN 442-2:2003. Radiators and convectors. In *Part 2: Test Methods and Rating*; Comite Europeen de Normalisation: Brussels, Belgium, 2003.

36. Remund, J.; Muller, S.C. *Solar Radiation and Uncertainty Information of Meteonorm 7*; PVSEC: Hamburg, Germany, 2011.

37. D'Agostino, D.; Zangheri, P.; Castellazzi, L. Towards Nearly Zero Energy Buildings in Europe: A Focus on Retrofit in Non-Residential Buildings. *Energies* **2017**, *10*, 117. [CrossRef]